PERGAMON

Scripta mater. 43 (2000) 417–422

Scripta MATERIALIA

www.elsevier.com/locate/scriptamat

ELECTROCHEMICAL CORROSION PROPERTIES OF AISI304 STEEL TREATED BY LOW-TEMPERATURE PLASMA IMMERSION ION IMPLANTATION

Xiubo Tian and Paul K. Chu*

Department of Physics & Materials Science, City University of Hong Kong, 83 Tat Chee Avenue, Kowloon, Hong Kong SAR, People's Republic of China

(Received January 11, 2000)
(Accepted in revised form April 25, 2000)

Keywords: Corrosion; Low-temperature; Implantation; Stainless steel

1. Introduction

For nitrogen-bearing alloys, nitrogen enrichment in the metal film surface and interface plays a significant role in inhibiting the anodic kinetics of metal dissolution (1). Ion implantation has been shown to be an effective technique to introduce a large amount of nitrogen into the materials in a controlled fashion to precisely modify the surface physical and chemical states. Plasma immersion ion implantation (PIII) (2–5) has recently emerged as the preferred method to implant nitrogen in niche applications. The technique circumvents the line-of-sight and retained dose limitation inherent to conventional beam-line ion implantation, and is thus particularly suitable for large components possessing non-planar and complex geometries. To enhance the tribological and corrosion properties of AISI304 steel, PIII experiments are typically conducted at elevated temperature to form thick enough expanded austenite in the top surface (6–9). However, low temperature treatment is more desirable in many applications but the corrosion properties of AISI304 after low temperature PIII has seldom been studied. Based on our literature search, only Mo containing AISI304L has been treated and investigated for the pitting corrosion resistance (10). In this work, we assess the electrochemical corrosion properties of low-temperature treated AISI304 steel in neutral chloride medium. Our results indicate the formation of three distinct layers after the treatment and that low temperature PIII is indeed effective in enhancing the corrosion resistance of the materials.

2. Experimental

AISI304 samples 30mm in diameter and 5mm thick were prepared. The composition of AISI304 steel is: 19wt% Cr, 9wt% Ni; 0.08wt% C, 2.0wt% Mn, 1.0wt% Si, 0.045wt% P, and 0.030wt% S (the balance being Fe). The samples were initially grounded and polished to attain a good surface finish. PIII was carried out in the multi-functional PIII instrument in the City University of Hong Kong (11). The nitrogen plasma was sustained by hot filament glow discharge, and the instrumental parameters are: plasma density = $3.0\times10^{15}/m^3$; implantation voltage = 30kV; pulsing frequency = 500Hz; pulse duration = 10μs, and treatment time = 3h. Good electrical and mechanical contact between the specimens and the oil-cooled sample chuck as well as the low ion flux used in our experiments induced very little temperature rise during the entire PIII treatment process.

PII: S1359-6462(00)00436-X

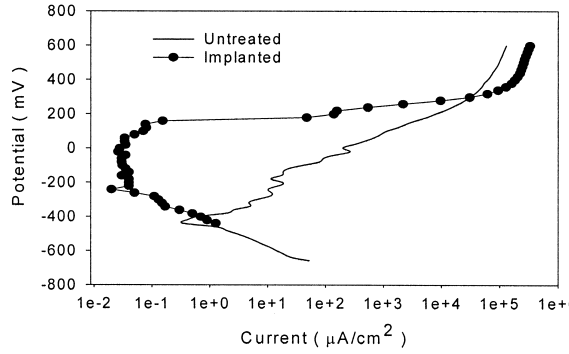

Figure 1. Potentiodynamic polarization curves acquired from the AISI304 samples in 3wt% NaCl solution.

The corrosion behavior of the samples was studied by electrochemical methods. A computer-assisted potentiostat (EG&G Par 273) was used to apply and scan the potential, and to display the data of the resulting potential-current curves. The polarization plots were acquired in an aerated 3% NaCl solution and the scanning rate for the polarization curve determination was 1mV/min. After the electrochemical tests, the sample surfaces were assessed by scanning electron microscopy (SEM). The elemental depth profiles were acquired by Auger electron spectroscopy using a PHI-610 SAM by bombarding with Ar ions and using an estimated average sputtering rate of 30nm/min. The phase structures were determined by glancing-angle x-ray diffraction using an X'pert-MRD system.

3. Results

The results of the electrochemical corrosion measurements are depicted in Fig. 1. The corrosion resistance is excellent, as demonstrated by a rather large shift of the equilibrium potential, very low corrosion current at the equilibrium potential, as well as a broad anodic zone of the low dissolution current. The pitting potential increases from −110mV to +150mV. It is projected to go even higher if the modified layers were thicker, for example at higher treatment temperature (12) or in a lower chloride content solution (13,14). The improvement originates from the chemical state change induced by ion bombardment. The morphology of the surface is shown in Fig. 2 and the enhanced corrosion resistance by low temperature PIII is corroborated. Pitting corrosion is observed and the materials just beneath the

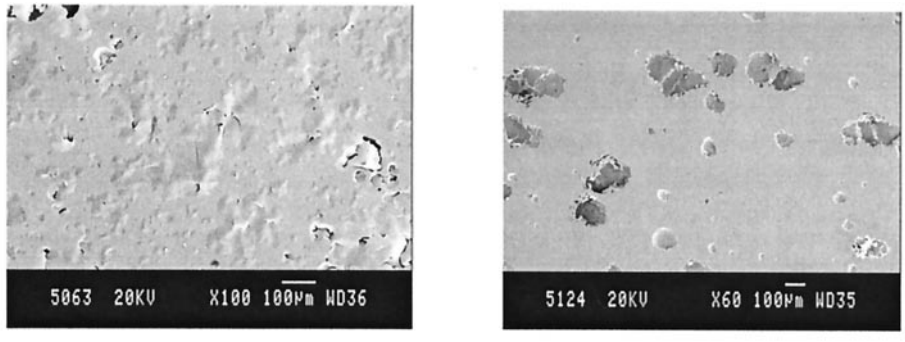

(a) (b)

Figure 2. Surface morphology after electrochemical corrosion of (a) untreated sample, and (b) implanted sample.

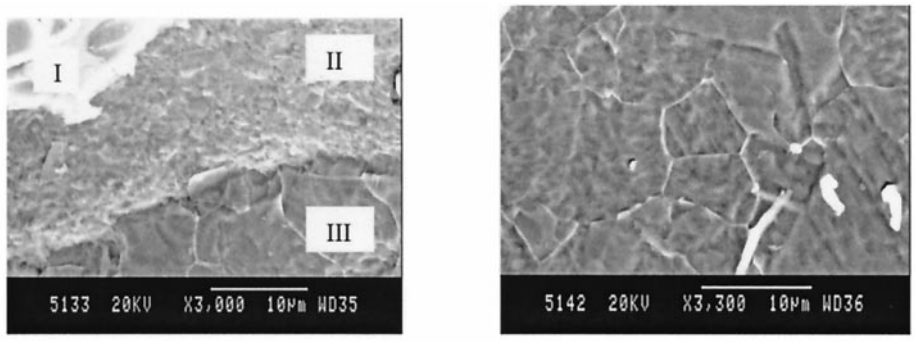

(a) (b)

Figure 3. SEM micrograph of a typical pit showing different layers: (a) whole view of three layers, and (b) the lowest layer.

top surface are preferentially dissolved leaving a thin film "floating" on the corrosion pits. As a result, the surface of the implanted and corroded sample resembles a platen with bubbles of different sizes. In contrast, the untreated sample is severely eroded in the same corrosion test. Pits can be observed on the entire surface, demonstrating the characteristics of uniform corrosion since the separate "floating" films have coalesced forming a big pitting area.

The SEM micrograph with a larger magnification elucidates an interesting phenomenon. As shown in Fig. 3, there exist three different zones in the corrosion pits implying chemical state changes along different depths after nitrogen PIII. The first surface section is the undestroyed top surface with a smooth appearance as shown in Fig. 2. The second layer results from uniform dissolution of the materials. The appearance of the third layer is considerably different from that of the other layers mentioned above, and the metallurgical morphology is indicated by the grain boundaries as shown in Fig. 3b. On the average, the third layer is slightly beneath or at the same depth as the second layer. Uniform corrosion has taken place in every grain, while the grain boundary is only slightly etched by the solution. Our interesting results thus unequivocally indicate that the grain boundaries have better corrosion resistance than the bulk of each grain. It is probably related to nitrogen transfer or Cr movement preferentially along the boundaries under the experimental conditions.

Grazing angle X-ray diffraction (GXRD) is used to examine new phases formed after low-temperature nitrogen PIII. The 5° XRD scans from the implanted austenitic AISI304 are exhibited in Fig. 4. No evident new phases can be observed in the implanted layer except the primary austenitic peaks, perhaps due to either the relatively large grazing angle or insufficient precipitates in the layer. That is, nitrogen PIII may yield a solid solution of nitrogen in the austenitic materials or tiny precipitate phases are immersed in the substrate (14). In fact, high-resolution studies show that there exist other oxide or nitride phases other than the Cr_2O_3 phase. Fe_3O_4, Fe_2O_3, FeO, CrN, Cr_2N, and others have been observed in implanted layers (14–16), although the layer containing the iron oxides is very thin (17).

The elemental depth profile of the implanted samples is displayed in Fig. 5. For comparison, the elemental composition in the top layer of the untreated AISI304 sample is shown on the right (17). The results reveal that the Cr fraction increases in the thin surface layer, and the maximum Cr content is 32at% that is 1.8 times that in the bulk. The oxygen profile shows a peak at the surface layer corresponding to the Cr-enriched layer (5nm). Comparing to the untreated sample, oxygen has penetrated to a depth more than 15nm indicating that low-temperature nitrogen PIII increases the thickness of the oxide layer. Our data are consistent with those demonstrated by other groups (18,19).

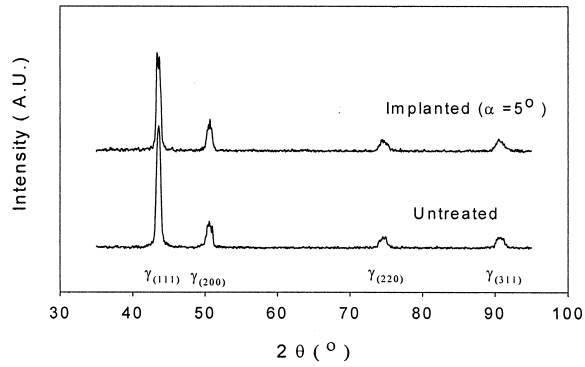

Figure 4. Grazing angle (5°) x-ray diffraction patterns acquired from the untreated and implanted samples.

Oxygen in the modified layers stems from the original oxide film on the sample surface recoiled into the substrate by energetic ion bombardment. There also exists a small amount of oxygen contamination in the residual vacuum of our instrument due to out-gassing and minor leaks in the gas lines. The oxygen molecules are ionized by the plasma and co-implanted into the substrate together with nitrogen ions. The Cr-rich layer also becomes markedly thicker as shown in Fig. 5b. Meanwhile, the Cr concentration decreases in the "nitrogen-ion-range" zone. Just beneath the Cr and O enriched layer, the Ni concentration shows a slight jump. These features are perhaps due to diffusion enhanced by ion irradiation and that different alloying elements have different affinity to oxygen. The ratio of oxygen to chromium indicates that iron oxides in addition to chromium oxides exist in the top layer because of a surplus of oxygen. However, as the oxygen concentration rapidly decreases, the iron oxide layer us speculated to be thinner as proposed by Nishimura et al. (17). The distribution of nitrogen exhibits a slightly distorted Gaussian shape with a peak depth of about 25nm and maximum concentration of 21at%. The nitrogen profile reaches a depth of 65nm (within Auger detection limit) indicating slight diffusion.

4. Discussion

It is generally accepted that the high corrosion resistance of stainless steel is due to the formation of a protective oxide-hydroxide film, and that Cr_2O_3 is responsible for the passive behavior (20,21). After

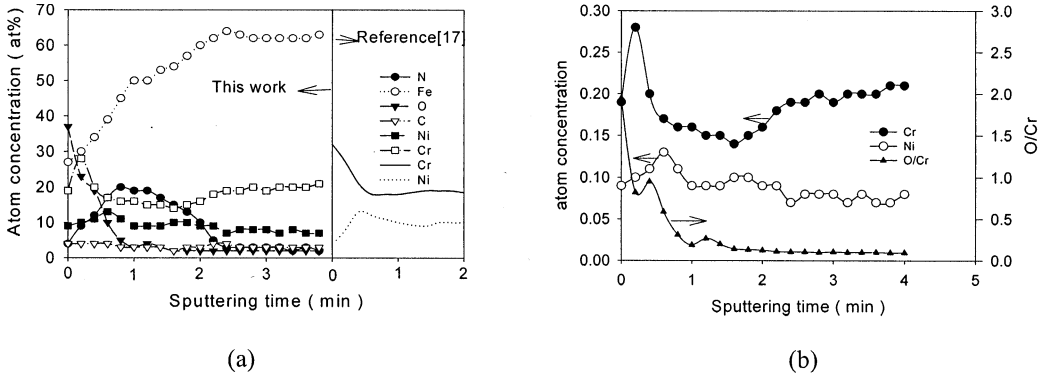

Figure 5. Auger depth profiles: (a) superimposed implanted sample (sputtering rate of 30nm/min) and untreated sample from Ref. (17) (equivalent sputtering rate of 10nm/min), (b) Cr, Ni and O profiles of the implanted sample.

PIII treatment, Cr is enriched in the top surface and oxygen has penetrated into the substrate, and so the layer containing Cr_2O_3 gets thicker (Fig. 5). This enhances the passive characteristics of the materials leading to improved corrosion resistance.

It is also known that nitrogen addition to austenitic stainless steels improves the pitting resistance. Several mechanisms have been proposed (15). For example, the rate of pH decrease in the pit nuclei by cathodic nitrogen dissolution: $N+4H^{+}+3e^{-}\rightarrow NH_4^{+}$ with possible repassivation is lower. The rate of this reaction is probably very low at high potential (for the implantation case). However, when a porous film is present in the pits, the applied potential drops mainly through this film whose thickness increases with the potential. The potential at the metal-salt interface is not altered and the reaction would then be kinetically possible. There is also an alternative mechanism due to the superficial enrichment in nitrogen. At high potential, the cathodic dissolution of nitrogen as NH_4^{+} will become too slow whereas the alloy dissolution will increase producing an enrichment in nitrogen. The mobile nitrogen atoms block some of the kink sites on the surface and the current density remains too small to initiate pits on the surface. In the presence of nitrogen, the rate of dissolution is higher for Fe and Ni than Mo and Cr. There is then surface enrichment in Cr and Mo leading to the formation of Cr and Mo mixed oxide films allowing the N enriched phase to passivate.

Based on our results, it is quite logical that low temperature nitrogen PIII leads to improvement in the corrosion resistance. Ion implantation not only increases the thickness of the layer containing Cr_2O_3 oxides but also makes nitrogen rich in the top surface. That is to say, the combined effects from oxygen and nitrogen induced by a single nitrogen ion implantation process mitigate the corrosion reaction.

Ion implantation changes the composition and structure in the near surface. Owing to the synergistic effects induced by ion implantation (nitrogen uptake, element diffusion, thermal evolution, etc.), different elements are enriched at different depths. Oxygen is the most enriched species in the top layer, and Cr is also abundant in the oxygen-rich zone. Nitrogen is enriched in the second zone corresponding to the ion range, but the Cr concentration is small. Finally, the modification mechanism of the third layer is linked to nitrogen diffusion and the long-range effects induced by ion implantation (22,23). Nitrogen diffusion can be inferred by its broad in-depth distribution as shown in the Auger depth profiles. Consequently, the corrosion resistance of each layer is considerably different and different corrosion behavior is demonstrated. In fact, this modified layer is quite thin and rapidly dissolves in usual electrochemical corrosion tests and the layer structure as well as corrosion characteristics are seldom observed in the pits. In this work, we are able to discern the different pitting behavior to elucidate the surface modification mechanism by low-temperature nitrogen plasma immersion ion implantation.

5. Conclusion

Although seldom investigated before, low-temperature nitrogen plasma immersion ion implantation improves the corrosion resistance of AISI304 stainless steel. The proposed technique, which is compatible to complex-shaped and large industrial components as well as applicable to niche applications in which low treatment temperature is required, is experimentally shown to not only make nitrogen rich in the top surface but also increase the thickness of the layer containing Cr_2O_3 oxides. Both effects synergistically mitigate surface corrosion reactions. Our experiments also show the interesting results that nitrogen PIII leads to enrichment of different elements along different depths, in particular oxygen. Consequently, a special layer structure with different chemical states as well as different corrosion behavior is observed at different depths.

Acknowledgments

The work was supported by Hong Kong Research Grants Council (RGC) Earmarked Grants 9040344 and 9040412, City University of Hong Kong Strategic Research Grant 7001028, as well as RGC/ Germany Joint Schemes 9050084 and 9050150.

References

1. Y. C. Lu and M. B. Ives, Corrosion Sci. 34, 1773 (1993).
2. J. R. Conrad, J. L. Radtke, R. A. Dodd, F. J. Worzala, and N. C. Tran, J. Appl. Phys. 2, 4951 (1987).
3. J. Tendys, I. J. Donnelly, M. J. Kenny, and J. T. A. Pollock, Appl. Phys. Lett. 53, 2143 (1988).
4. S. Mandl, N. P. Barradas, J. Brutsher, R. Guenzel, and W. Moeller, Nucl. Instrum. Meth. B. 127/128, 996 (1997).
5. P. K. Chu, X. Lu, S. S. K. Iyer, and N. W. Cheung, Solid State Technol. 40(5), S9 (1997).
6. M. Samandi, B. A. Shedden, D. I. Smith, G. A. Collins, R. Hutchings, and J. Tendys, Surf. Coat. Technol. 59, 261 (1993).
7. G. A. Collins, R. Hutchings, K. T. Short, J. Tendys, X. Li, and M. Samandi, Surf. Coat. Technol. 74, 417 (1995).
8. X. B. Tian, Z. M. Zeng, B. Y. Tang, T. K. Kwok, and P. K. Chu, International Conference on Surface Modification of Metals by Ion Beams (SMMIB99), Beijing, China, September 19–24 (1999).
9. X. B. Tian, Z. M. Zeng, T. Zhang. B. Y. Tang, and P. K. Chu, Thin Solid Films. in press.
10. P. P. Smith, R. A. Buchanan, J. R. Roth, S. G. Kamath, J. Vac. Sci. Technol. B12, 940 (1994).
11. P. K. Chu, B. Y. Tang, Y. C. Cheng, and P. K. Ko, Rev. Sci. Instrum. 68(4), 1866 (1997).
12. M. K. Lei and Z. L. Zhang, J. Vac. Sci. Technol. A1592, 421 (1997).
13. A. J. Sedriks, Corrosion of Stainless Steels, John Wiley, New York (1996).
14. Y. J. Geng, D. H. Wang, B. Q. Chen, and F. Z. Cui, J. Phys. D Appl. Phys. 280, 226 (1995).
15. R. Sabot, R. Devaux, A. M. de Becdelievre and C. Duret-Thual, Corros. Sci. 33, 1121 (1992).
16. P. Marcus and M. E. Bussell, Appl. Surf. Sci. 59, 7 (1992).
17. O. Nishimura, K. Yabe, K. Saito, T. Yamashina, and M. Iwaki, Surf. Coat. Technol. 66, 403 (1994).
18. B. Garke, Chr. Edelmann, R. Guenzel, and J. Brutscher, Surf. Coat. Technol. 93, 318 (1997).
19. D. Weng and M. Wang, Mater. Chem. Phys. 54, 338 (1998).
20. A. Hannani and F. Kermiche, Trans. IMF. 76, 114 (1998).
21. P. Marcus and E. Protopopoff, J. Electrochem. Soc. 137, 2709 (1990).
22. A. N. Didenko, E. V. Kozlov, Y. P. Sharkeev, A. S. Tailashev, A. I. Rjabchikov, L. Pranjavichus, and L. Augulis, Surf. Coat. Technol. 56, 97 (1993).
23. Y. P. Sharkeev, E. V. Kozlov, A. N. Didenko, S. N. Kolupaeva, and N. A. Vihor, Surf. Coat. Technol. 83, 15 (1996).